

# An approach to analysis of dynamic crack growth at bimaterial interface

R.Nikolic \* Jelena M. Djokovic †

## Abstract

In this paper is presented the new approach to asymptotic analysis of the stress and strain fields around a crack tip that is propagating dynamically along a bimaterial interface. Through asymptotic analysis the problem is being reduced to solving the Riemann-Hilbert's problem, what yields the strain potential that is used for determination of the strain field around a crack tip. The considered field is that of a dynamically propagating crack with a speed that is between zero and shear wave speed of the less stiffer of the two materials, bound along the interface. Using the new approach in asymptotic analysis of the strain field around a tip of a dynamically propagating crack and possibilities offered by the Mathematica programming package, the results are obtained that are compared to both experimental and numerical results on the dynamic interfacial fracture known from the literature. This comparison showed that it is necessary to apply the complete expression obtained by asymptotic analysis of optical data and not only its first term as it was done in previous analyses.

**Keywords:** Interfacial crack, dynamic crack growth, Mathematica®

---

\*Faculty of Mechanical Engineering, Sestre Janjic 6, 34000 Kragujevac, Serbia

†Technical Faculty of Bor, University of Belgrade, Vojske Jugoslavije 12, 19210 Bor, Serbia

## 1 Introduction

Scientific explanation of the initiation and growth mechanisms of a crack on a bimaterial interface is fundamental for understanding the fracture process in materials like composites and ceramics. The very important mechanism of fracture of fiber-reinforced composites and whisker-reinforced ceramics is, for instance, debonding between the substrate and reinforcing phases. This failure process can be quasi-static or dynamic, depending on the type of loading to which the composite structure is subjected.

The interfacial crack lies between the two ideally bound elastic half spaces. Williams (1959) published first papers on that subject. He studied local stress field near the tip of the traction free semi-infinite interfacial crack. Williams has noticed that, as opposite to homogeneous materials, stresses for a crack on the interface exhibit the oscillatory character. Many authors have followed his work, and papers were published on the problem of the static growth of an interfacial crack. The well known are works by Sih and Rice (1964) and Rice and Sih (1965), who obtained explicit expressions for stress field in the vicinity of a crack tip, and accordingly, the far elastic stress fields for different problems. Papers by Erdogan (1965), England (1965) and Malyshev and Salganik (1965) provided the new contribution to research of the two-dimensional singular model for single or several cracks in bimaterial systems. More recently, papers of Rice (1988), Hutchinson and Suo (1992) and Shih (1991) provided for progress in research of static interfacial fractures.

The failure process can also be dynamic, what leads to necessity of analyzing the dynamic crack growth on bimaterial interface. Due to complexity of the problem, only a few theoretical results exist. They all provided solutions only for particular fracture problems, as stated by Liu, Lambros and Rosakis (1993). Those results provided insight of the dynamic crack behavior only in the immediate vicinity of the crack tip. Obviously, the knowledge of the complete spatial structure of the stress field, around the moving interfacial crack tip is necessary.

Therefore, while the theoretical investigations were still lagging, numerous experimental investigations of the strain field around an interfacial crack tip were conducted. The most famous results were by Tippur and Rosakis (1991) and Rosakis, Lee and Lambros (1991) using the optical method *Coherent Gradient Sensor (CGS)* and very high-speed photogra-

phy. They used polymethylmetacrylate (PMMA) / Al as the bimaterial system. The considered speeds were up to 90 % of Rayleigh's wave speed for PMMA. Guided by this investigation, Yang, Suo and Shih (1991) obtained structure of the elastodynamic field in steady state growth conditions of an interfacial crack. In addition, inspired by experiments by Tippur and Rosakis (1991), Lo, Nakamura and Kushner (1994) have conducted a numerical analysis of the same bimaterial system that was used in experiments.

The experimental research described in work by Liu, Lambros and Rosakis (1993) assume accelerations in the crack tip and very high crack growth speed. Existence of acceleration creates conditions in which application of the uniform crack growth assumption is not adequate. In this paper is given the asymptotic structure of the near tip fields for a crack in bimaterial system, for the non-uniform crack growth. Works of Freund (1990) and Freund and Rosakis (1992) that were treating the problem of the non-uniform crack growth under the Mode I loading in homogeneous isotropic material preceded the paper by Rosakis, Lee and Lambros (1991). Liu and Rosakis (1994) applied the same procedure for the non-uniform crack growth in the mixed mode for homogeneous isotropic material along an arbitrary curved path.

In section two of this paper is presented the general formulation of the problem. The interfacial parameters characteristics are presented in section three. They depend on characteristics of the bimaterial combination and crack tip speed. Section four gives the asymptotic elastodynamic field around the interfacial crack tip. This formulation follows closely that of Liu, Lambros and Rosakis (1993). The idea was to compare their results and those of Singh et al. (1997), obtained by the optical method *Coherent Gradient Sensor (CGS)* and very high speed photography, with our results obtained analytically by application of the programming package *Mathematica* presented in section five, Veljkovic (1998, 2001) and Nikolic and Veljkovic (2002, 2004). *Mathematica* is used for solving the non-uniform elastodynamic field. In this way, the analytical results are obtained, which are used for quantitative analysis of optical interferographs of dynamic experiments on bimaterial systems. Possibilities offered by *Mathematica* enable "accurate" calculations. Since here the subject of simulation is actually an asymptotic expression, it is not "solved" completely accurately, but its presentation by *Mathematica* is much better, or closer to "accu-

rate”, than by application of any numerical method. Section six presents discussion of results and the comparison with experimental data and offers concluding remarks.

## 2 Formulation of the problem

For dynamical problem, the equations of motion are used instead of equilibrium equations what gives the following:

$$\frac{\partial \sigma_{ji}}{\partial x_j} = \rho \ddot{u}_i, \quad (1)$$

where  $x_j$  are the orthogonal coordinates, ( $j = 1, 2$ ) and dot indicates the time derivative, Anderson (1991). For the quasi-static problems, the term on the right hand side of (1) vanishes. For a linear elastic material, it is possible to write the equations of motion in terms of displacements and elastic constants, with introducing the compatibility equations and stress-strains relationship:

$$\mu \frac{\partial^2 u_i}{\partial x_j \partial x_j} + (\lambda + \mu) \frac{\partial^2 u_i}{\partial x_i \partial x_j} = \rho \ddot{u}_i, \quad (2)$$

where  $\mu$  and  $\lambda$  are the Lamé constants.

Considered is the planar body that consists of two homogeneous, isotropic, linearly elastic materials that are bonded along a linear interface. The crack propagates non-uniformly along the interface, Figure 1.

The usual fixed Cartesian coordinate system  $(x_1, x_2)$  is introduced in such a way that the  $x_1$ -axis lies on the interface and coincides with the crack growth direction, and the  $x_2$  axis is perpendicular to the crack plane. It is assumed that the crack propagates non-uniformly with speed  $v(t)$ , and that the crack surfaces are traction free. At time moment  $t = 0$ , the crack tip is in the reference frame origin, thus the crack growth in time  $t \geq 0$  is characterized by length  $\ell(t)$ , ( $v(t) = \dot{\ell}(t)$ ), which represents the distance from the origin to the crack tip. The moving coordinate system is such that its origin is at the crack tip and the standard relations between the systems' coordinates are given by:

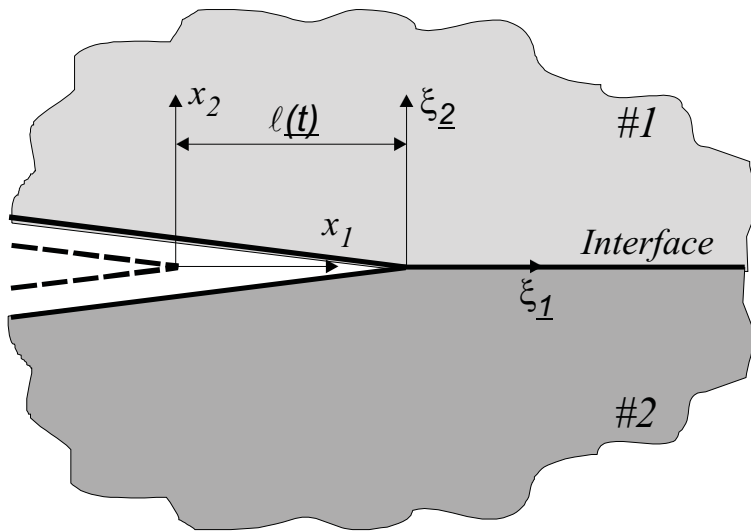


Figure 1: Schematic representation of the dynamic crack growth along a bimaterial interface

$$\xi_1 = x_1 - \ell(t), \quad \xi_2 = x_2. \tag{3}$$

If one assumes the plane strain state for each of the two materials that constitute the interface, the displacement field can be described by two displacement potentials  $\phi_k(x_1, x_2, t)$  and  $\psi_k(x_1, x_2, t)$ , where the subscript  $k$  refers to materials 1 and 2, respectively. In Figure 1, material 1 is shown above, while the material 2 is below the interface. Accordingly, in each of the two materials the displacement components can be expressed as:

$$u_\alpha(x_1, x_2, t) = \phi_{,\alpha}(x_1, x_2, t) + e_{\alpha\beta}\psi_{,\beta}(x_1, x_2, t), \tag{4}$$

where  $\alpha, \beta \in \{1, 2\}$ ,  $\{ \}_{,\alpha}$  denote differentiation with respect to coordinate and the summation convention holds, and  $e_{\alpha\beta}$  is the two-dimensional symbol defined as:  $e_{12} = -e_{21} = 1, e_{11} = e_{22} = 0$ . Substituting (4) into (3), one obtains:

$$\begin{aligned} \phi_{,\alpha\alpha}(x_1, x_2, t) - \frac{1}{c_\ell^2}\ddot{\phi}(x_1, x_2, t) &= 0 \\ \psi_{,\alpha\alpha}(x_1, x_2, t) - \frac{1}{c_s^2}\ddot{\psi}(x_1, x_2, t) &= 0 \end{aligned} \tag{5}$$

where:  $\mu$  – is the shear modulus, and  $c_\lambda$  and  $c_s$  are the longitudinal and

shear wave speed for materials above and below the interface, respectively. Those speeds are, for each of the two materials, in terms of shear modulus  $\mu$ , density  $\rho$  and Poisson's ratio  $\nu$ , defined as:

$$c_\ell = \sqrt{\frac{\kappa + 1}{\kappa - 1} \cdot \frac{\mu}{\rho}}, \quad c_s = \sqrt{\frac{\mu}{\rho}}, \quad (6)$$

where:  $\kappa = 3 - 4\nu$  for the plane strain state and  $\kappa = (3 - \nu)/(1 + \nu)$  for the plane stress state.

The stress components are expressed as functions of the displacement potentials, as

$$\begin{aligned} \sigma_{11} &= \mu \left[ \frac{c_\ell^2}{c_s^2} \phi_{,11} - 2\phi_{,22} + 2\psi_{,12} \right] \\ \sigma_{22} &= \mu \left[ \frac{c_\ell^2}{c_s^2} \phi_{,22} - 2\phi_{,11} - 2\psi_{,12} \right] \\ \sigma_{12} &= \mu [2\phi_{,12} + \psi_{,22} - \psi_{,11}] \end{aligned} \quad (7)$$

for each of the considered materials.

In the moving reference frame, equations of motion (5) can be expressed, in terms of the displacement potentials  $\phi(x_1, x_2, t)$  and  $\psi(x_1, x_2, t)$  become:

$$\begin{cases} \left(1 - \frac{v^2(t)}{c_\ell^2}\right) \phi_{,11} + \phi_{,22} + \frac{\dot{v}(t)}{c_\ell^2} \phi_{,1} + \frac{2v(t)}{c_\ell^2} \phi_{,1t} - \frac{1}{c_\ell^2} \phi_{,tt} = 0 \\ \left(1 - \frac{v^2(t)}{c_s^2}\right) \psi_{,11} + \psi_{,22} + \frac{\dot{v}(t)}{c_s^2} \psi_{,1} + \frac{2v(t)}{c_s^2} \psi_{,1t} - \frac{1}{c_s^2} \psi_{,tt} = 0 \end{cases} \quad (8)$$

It is assumed that  $\phi(\xi_1, \xi_2, t)$  and  $\psi(\xi_1, \xi_2, t)$ , for each material, can be represented in the form of series:

$$\begin{aligned} \phi(\xi_1, \xi_2, t) &= \sum_{m=0}^{\infty} \gamma^{p_m} \phi_m(\eta_1, \eta_2, t) \\ \psi(\xi_1, \xi_2, t) &= \sum_{m=0}^{\infty} \gamma^{p_m} \psi_m(\eta_1, \eta_2, t) \end{aligned} \quad \text{when } r = \sqrt{\xi_1^2 + \xi_2^2} \rightarrow 0, \quad (9)$$

where:  $\eta_i = \xi_i/\gamma$ ,  $\alpha \in \{1, 2\}$  and  $\gamma$  is the small arbitrary number. The parameter  $\gamma$  is used in order to extend the area around the crack tip to the whole field. If  $\gamma$  is chosen as infinitely small, all points in the  $(\xi_1, \xi_2)$  plane, except for those that are in the immediate vicinity of the crack tip, are out of the consideration area in the  $(\eta_1, \eta_2)$  plane and the crack tip lies along the whole negative part of the  $\eta_1$  axis. If one adopts that  $\gamma = 1$ , the above equations (9) would be the asymptotic presentation of the displacement potential in the non-scaled physical plane for each material, respectively.

In the asymptotic presentation (9), the influence of  $\gamma$  is such that:

$$p_{m+1} = p_m + \frac{1}{2}, \quad m = 0, 1, 2, \dots \quad (9)$$

The displacement will be limited, over the whole area, but stresses could be singular at the crack tip, it is expected that  $p_0$  will be within the range  $1 \leq p_0 \leq 2$ . It also holds:

$\frac{\varepsilon^{p_{m+n}} \phi_{m+n}(\eta_1, \eta_2, t)}{\varepsilon^{p_m} \phi_m(\eta_1, \eta_2, t)} \rightarrow 0$ , when  $\gamma \rightarrow 0$ , (11) for any positive number  $n$ . If the non-scaled physical plane is adopted, it would be:

$\frac{\phi_{m+n}(\xi_1, \xi_2, t)}{\phi_m(\xi_1, \xi_2, t)} \rightarrow 0$ , when  $r = \sqrt{\xi_1^2 + \xi_2^2} \rightarrow 0$ , (12) for any positive number  $n$ , thus in the physical plane  $(\xi_1, \xi_2)$  is  $\phi_m(\xi_1, \xi_2, t)$  determined according to its contribution to strain field at the crack tip. These characteristics of  $\phi_m$  are also valid for  $\psi_m$ .

If the asymptotic representation of  $\phi(\xi_1, \xi_2, t)$  and  $\psi(\xi_1, \xi_2, t)$ , equations (9), is substituted into Equation (8), the two equations are obtained, whose left hand sides represent the infinite series in  $\gamma$  and the right hand sides vanish. If  $\gamma$  is the arbitrary number, the coefficient of each term with  $\gamma$  will be equal to zero. Thus, the equations of motion are reduced to series of coupled differential equations for  $\phi_m(\eta_1, \eta_2, t)$  and  $\psi_m(\eta_1, \eta_2, t)$ , Liu, Lambros and Rosakis (1993):

$$\begin{aligned} \phi_{m,11} + \frac{1}{\alpha_\ell^2(t)} \phi_{m,22} &= -\frac{2\sqrt{v(t)}}{\alpha_\ell^2(t)c_\ell^2} \left\{ \sqrt{v(t)} \phi_{m-2,1} \right\}_{,t} + \frac{1}{\alpha_\ell^2(t)c_\ell^2} \phi_{m-4,tt} \\ \psi_{m,11} + \frac{1}{\alpha_s^2(t)} \psi_{m,22} &= -\frac{2\sqrt{v(t)}}{\alpha_s^2(t)c_s^2} \left\{ \sqrt{v(t)} \psi_{m-2,1} \right\}_{,t} + \frac{1}{\alpha_s^2(t)c_s^2} \psi_{m-4,tt} \end{aligned} \quad (10)$$

for  $m = 0, 1, 2, \dots$ , and values of  $\alpha_\lambda$  and  $\alpha_s$  depend on the vicinity of the crack tip and time  $t$ , by:

$$\alpha_{\ell,s}^2 = 1 - \frac{v^2(t)}{c_{\ell,s}^2}. \quad (11)$$

The expression "coupled" is used in the sense that the higher order solutions for  $\phi_m$  and  $\psi_m$  will depend on the lower order solution for the same variables. Equations are not coupled only in the case when  $m = 0$  and  $m = 1$ , Liu, Lambros and Rosakis (1993). For the case when  $m \geq 1$ , from equations (10) can be seen that solutions for  $\phi_m$  and  $\psi_m$  consist of two parts. One is the particular solution, which is completely defined by the

lower order solutions for  $\phi_m$  and  $\psi_m$ . The second part is the homogeneous solution that satisfies the Laplace's equation in the corresponding scaled coordinate plane. Combination of particular and homogeneous solutions must satisfy the boundary conditions on the crack faces and along the interface.

Liu, Lambros and Rosakis (1993) have found the solutions for  $\phi_m$  and  $\psi_m$  (expression (13), p. 1894 and (54), p. 1903). Associated with solutions for  $\phi_m$  and  $\psi_m$  they determined the stress components (expressions (56), (57) and (58), p. 1905). Their equations make good use to determine the angular variations of stresses for different values of crack tip speed in the PMMA/steel bimaterial system. In Figures 2 and 3 are presented results of simulation by *Mathematica* of those expressions.

### 3 Characteristic parameters of the dynamic interfacial fracture

In analysis of an interfacial crack that propagates dynamically along the interface, there exist two parameters, which do not depend only on characteristics of materials that form the bimaterial system, but also on the crack tip speed. These parameters were defined earlier; see for instance Yang, Suo and Shih (1991). Characteristics of these parameters are very important, since the asymptotic field in the crack tip changes drastically in their presence. The first of these parameters is defined as:

$$\varepsilon = \frac{1}{2\pi} \ln \frac{1 - \beta}{1 + \beta}, \quad (12)$$

where:  $\beta = \frac{h_{11}}{\sqrt{h_{12}h_{21}}}$ , while the second is defined with:

$$\eta = \sqrt{\frac{h_{21}}{h_{12}}}. \quad (13)$$



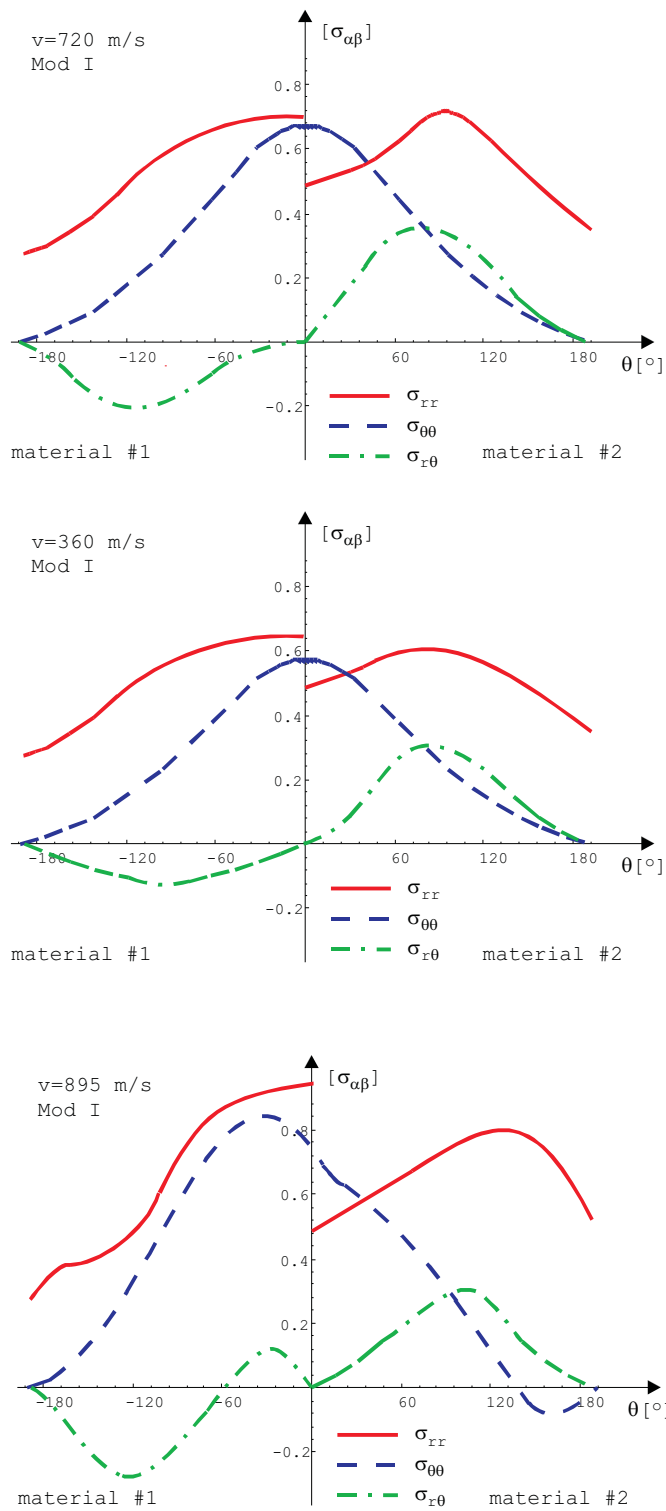


Figure 2: Angular variations of stresses for different values of crack tip speed in a PMMA/steel bimaterial system under the Mode I load, using Mathematica.

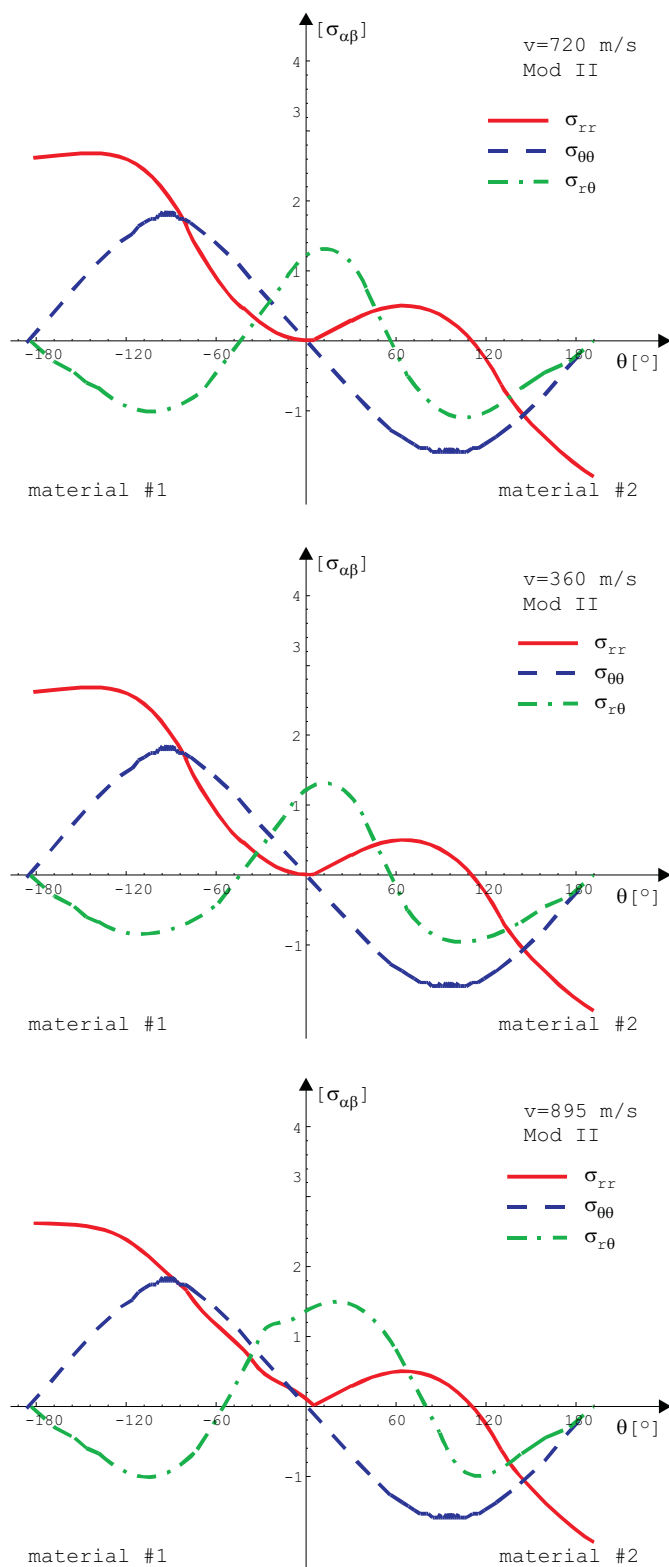


Figure 3: Angular variations of stresses for different values of crack tip speed in a PMMA/steel bimaterial system under the Mode II, using *Mathematica*.

In definitions of parameters (12) and (13) the auxiliary functions are:

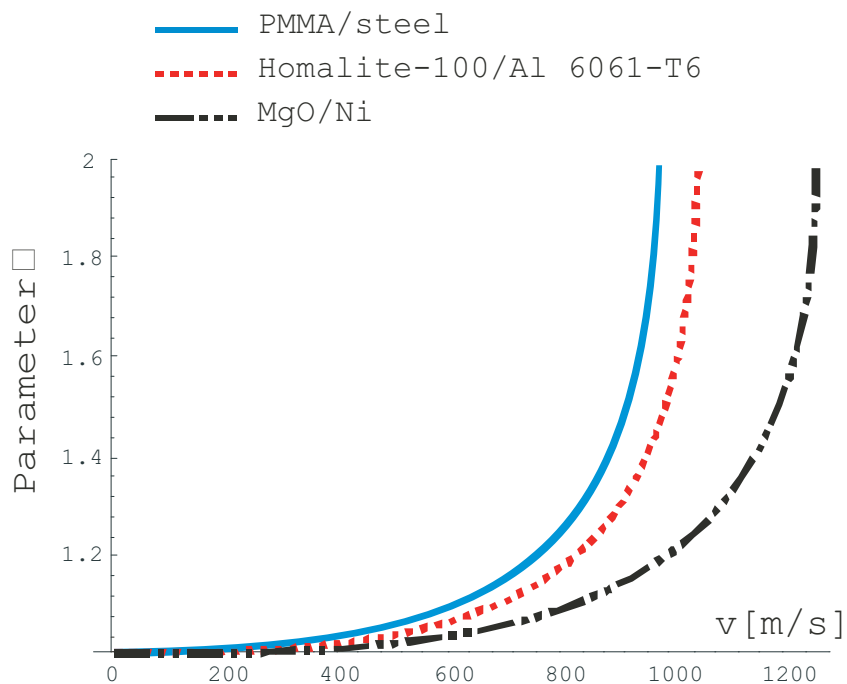
$$\begin{aligned}
 h_{11} &= \left\{ \frac{2\alpha_\ell\alpha_s - (1+\alpha_s)^2}{\mu D(v)} \right\}_1 - \left\{ \frac{2\alpha_\ell\alpha_s - (1+\alpha_s)^2}{\mu D(v)} \right\}_2 \\
 h_{12} &= \left\{ \frac{\alpha_s(1-\alpha_s)^2}{\mu D(v)} \right\}_1 - \left\{ \frac{\alpha_s(1-\alpha_s)^2}{\mu D(v)} \right\}_2 \\
 h_{21} &= \left\{ \frac{\alpha_\ell(1-\alpha_s)^2}{\mu D(v)} \right\}_1 - \left\{ \frac{\alpha_\ell(1-\alpha_s)^2}{\mu D(v)} \right\}_2,
 \end{aligned} \tag{14}$$

where:  $D(v) = 4\alpha_\ell\alpha_s - (1 + \alpha_s^2)^2$ .

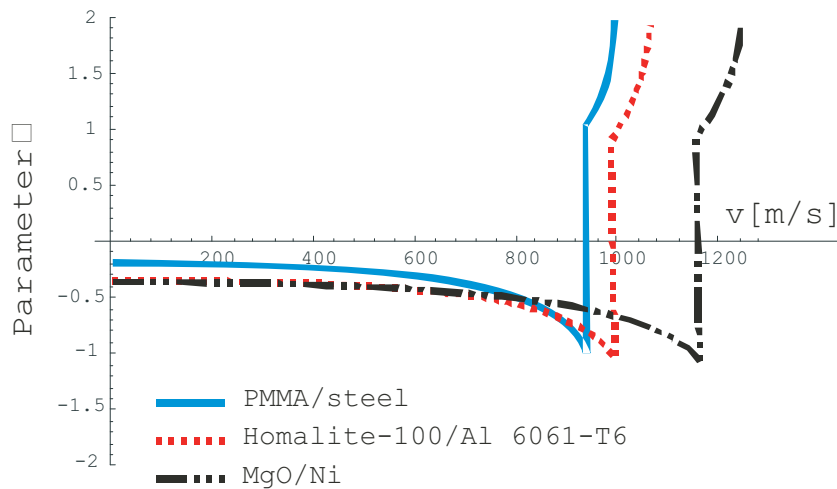
In Figure 4 are shown variations of parameters  $\eta$  and  $\beta$  as functions of the crack tip speed for the plane strain conditions for three different bimaterial combinations. Diagrams shown in Figures 4(a) and 4(b) are drawn by application of the *Mathematica* programming package. It can be seen that parameters  $\eta$  and  $\beta$  depend weakly on materials disagreement but strongly on the crack speed. It can further be noticed that the parameter  $\eta$  changes smoothly, from 1 for the stationary interfacial crack, to  $\infty$ , when the crack tip speed approaches transversal wave speed for material 1. However, the situation is quite different for the other parameter,  $\beta$ . When the crack tip speed is less than the Rayleigh's wave speed for material 1, i.e.,  $c_R^{(1)}$ , the parameter  $\beta$  changes smoothly and tends to -1, when the crack tip speed is very close to  $c_R^{(1)}$ . When the crack tip speed becomes equal to  $c_R^{(1)}$ ,  $D_1(v)$  changes its sign and parameter  $\beta$  has a jump from -1 to 1 and further tends to  $\infty$ , when the crack tip velocity approaches the wave speed of material 1.

## 4 Asymptotic elastodynamic field around an interfacial crack that propagates non-uniformly

The following section is partially taken from Liu, Lambros and Rosakis (1993), and thus presented here in the abbreviated version. The objective is to get the expression for the first stress invariant and its derivative with respect to coordinate  $x_1$  and than to calculate it with application of the programming package *Mathematica*. The point is to illustrate the necessity of taking into account the whole expression for the derivative, and not only its leading term, as was the case in Yang, Suo and Shih



(a) Variation of parameter  $\eta$  with speed for the plane strain conditions for three different bimaterial combinations



(b) Variation of parameter  $\beta$  with speed for the plane strain conditions for three different bimaterial combinations.

Figure 4:

(1991). Liu, Lambros and Rosakis (1993) came to the same conclusion, but their simulations are done numerically, and thus are presumably less “accurate”. Both expressions (from Yang, Suo and Shih (1991) and Liu, Lambros and Rosakis (1993)) are simulated in this paper by *Mathematica* and results are presented and compared in section five.

Liu, Lambros and Rosakis (1993) argue that for the sake of comparison with experimental investigations, the asymptotic analysis should be conducted only of the first stress invariant around the interfacial crack tip. Let, for any complex function  $W(t)$ , the intensity be denoted with  $|W|$  and phase with  $\Phi(W)$ . Let the scaled polar coordinate system  $(r_\lambda, \theta_\lambda)$ , with the origin at the moving crack tip be defined with:

$$r_\ell = \sqrt{\xi_1^2 + \alpha_\ell^2 \xi_2^2}, \quad \theta_\ell = \arctg \frac{\alpha_\ell \xi_2}{\xi_1}. \tag{15}$$

The first stress invariant in material above the interface can be expressed as:

$$\begin{aligned} \frac{\sigma_{11} + \sigma_{22}}{2\mu(\alpha_\ell^2 - \alpha_s^2)} = & |A_0(t)| \left\{ \Sigma_0(\theta_\ell) \cos(\varepsilon \ln r_\ell) + \sum_0^*(\theta_\ell) \sin(\varepsilon \ln r_\ell) \right\} \frac{1}{\sqrt{r_\ell}} \\ & + \frac{4\alpha_s}{\mu D(v)(1 + \omega_s)} |A_1(t)| \cos(\Phi(A_1)) \\ + \dot{\varepsilon} \left\{ \Sigma_d(\theta_\ell) \cos(\varepsilon \ln r_\ell) + \sum_d^*(\theta_\ell) \sin(\varepsilon \ln r_\ell) \right\} & \sqrt{r_\ell} (\ln r_\ell)^2 \\ + \left\{ \Sigma_t(\theta_\ell) \cos(\varepsilon \ln r_\ell) + \sum_t^*(\theta_\ell) \sin(\varepsilon \ln r_\ell) \right\} & \sqrt{r_\ell} \ln r_\ell \\ + \left\{ \Sigma_{tt}(\theta_\ell) \cos(\varepsilon \ln r_\ell) + \sum_{tt}^*(\theta_\ell) \sin(\varepsilon \ln r_\ell) \right\} & \sqrt{r_\ell} \\ + |A_2(t)| \left\{ \Sigma_2(\theta_\ell) \cos(\varepsilon \ln r_\ell) + \sum_2^*(\theta_\ell) \sin(\varepsilon \ln r_\ell) \right\} & \sqrt{r_\ell} + O(r_\ell) . \end{aligned} \tag{16}$$

This equation corresponds to (88, p. 1916) of Liu, Lambros and Rosakis (1993), and all the coefficients are defined there. The discussion following that equation should not be given here, except for stressing that the first term has properties of the square root and is of the oscillatory nature. This corresponds to the complex dynamic stress intensity factor  $K^d(t)$ , which was defined by Yang, Suo and Shih (1991). It is important to emphasize that the influence of the non-uniform crack growth can noticeably change

the structure of  $r$  and  $\theta$  fields from that predicted by the steady-state growth approximation.

The first stress invariant, differentiated with respect to  $x_1$  in the material above the interface can be expressed as:

$$\begin{aligned} \frac{(\sigma_{11} + \sigma_{22})_{,1}}{2\mu(\alpha_\ell^2 - \alpha_s^2)} = & |A_0(t)| \left\{ \Pi_0(\theta_\ell) \cos(\varepsilon \ln r_\ell) + \overset{*}{\Pi}_0(\theta_\ell) \sin(\varepsilon \ln r_\ell) \right\} r_\ell^{-3/2} \\ & + \dot{\varepsilon} \left\{ \Pi_d(\theta_\ell) \cos(\varepsilon \ln r_\ell) + \overset{*}{\Pi}_d(\theta_\ell) \sin(\varepsilon \ln r_\ell) \right\} \frac{1}{\sqrt{r_\ell}} (\ln r_\ell)^2 \\ & + \left\{ \Pi_t(\theta_\ell) \cos(\varepsilon \ln r_\ell) + \overset{*}{\Pi}_t(\theta_\ell) \sin(\varepsilon \ln r_\ell) \right\} \frac{1}{\sqrt{r_\ell}} \ln r_\ell \\ & + \left\{ \Pi_{tt}(\theta_\ell) \cos(\varepsilon \ln r_\ell) + \overset{*}{\Pi}_{tt}(\theta_\ell) \sin(\varepsilon \ln r_\ell) \right\} \frac{1}{\sqrt{r_\ell}} \\ & + |A_2(t)| \left\{ \Pi_2(\theta_\ell) \cos(\varepsilon \ln r_\ell) + \overset{*}{\Pi}_2(\theta_\ell) \sin(\varepsilon \ln r_\ell) \right\} \frac{1}{\sqrt{r_\ell}} + O(r_\ell) . \end{aligned} \quad (17)$$

Equation (17) corresponds to Equation (109, p. 1935) of Liu, Lambros and Rosakis (1993). As stated in that paper, Equation (17) has four orders of the variable  $r_\lambda$ . Those are  $r_\ell^{-3/2}$ ,  $r_\ell^{-1/2}(\ln r_\ell)^2$ ,  $r_\ell^{-1/2} \ln r_\ell$  and  $r_\ell^{-1/2}$ . There are 28 unknown constants here. The first two constants  $|A_0|$  and  $\Phi(A_0)$  correspond to the complex dynamic stress intensity factor  $K^d(t)$  defined by Yang, Suo and Shih (1991). Actually, the simplest term in (17) is reduced to equation obtained by Yang, Suo and Shih (1991):

$$\begin{aligned} \frac{\partial(\widehat{\sigma}_{11} + \widehat{\sigma}_{22})}{\partial x_1} = & \frac{r_\ell^{-3/2} e^{-\varepsilon(\pi - \theta_\ell)} A(t)}{2\sqrt{2\pi}} \left\{ (1 + \alpha_s^2 - 2\eta\alpha_s) e^{2\varepsilon(\pi - \theta_\ell)} \cos\left(\frac{3\theta_\ell}{2} - \Phi(t) - \varepsilon \ln r_\ell\right) \right. \\ & - (1 + \alpha_s^2 + 2\eta\alpha_s) \cos\left(\frac{3\theta_\ell}{2} + \Phi(t) + \varepsilon \ln r_\ell\right) \\ & + 2\varepsilon (1 + \alpha_s^2 - 2\eta\alpha_s) e^{2\varepsilon(\pi - \theta_\ell)} \sin\left(\frac{3\theta_\ell}{2} - \Phi(t) - \varepsilon \ln r_\ell\right) \\ & \left. - 2\varepsilon (1 + \alpha_s^2 + 2\eta\alpha_s) \sin\left(\frac{3\theta_\ell}{2} + \Phi(t) + \varepsilon \ln r_\ell\right) \right\} , \end{aligned} \quad (18)$$

where:

$$A(t) = \frac{(\alpha_\ell^2 - \alpha_s^2) |K^d(t)|}{D(v)ch(\varepsilon\pi)}, \quad K^d(t) = K_1^d(t) + iK_2^d(t), \quad \Phi(t) = \arctg \frac{K_2^d(t)}{K_1^d(t)} .$$

The first four terms in Equation (17) have the same form as those obtained in the equilibrium state conditions. However, the other terms

are much more complex and possess some unusual characteristics. They have the proportionality coefficient  $\dot{\varepsilon} = \varepsilon'(v)\dot{v}(t)$ . If  $\dot{\varepsilon} = 0$  the majority, but not all, terms of Equation (17) vanish, since they depend on the time derivative of the complex dynamic stress intensity factor and the crack tip speed.

## 5 Results and discussion

To demonstrate necessity of analysis presented in section 4, in presentation of experimental data will be analyzed the case of a non-uniformly propagating crack.

Results obtained by application of programming routine *Mathematica* for numerically evaluated Equations (17) and (18) are shown in Figure 5. Considering the possibilities offered by programming package *Mathematica*, the stress field, shown in Figure 5(a) presents the analytical “solution” of Equation (17). In obtaining the contour diagrams in Figures 5 and 6, coordinates  $x_1$  and  $x_2$  were scaled with  $L = 1$  m since the logarithmic function  $\ln r_\ell$  ought to be dimensionless. This was discussed by Rice (1988). In the asymptotic analysis, it was supposed that the length  $L$  could be arbitrary. The value of the complex dynamic factor,  $K^d(t)$ , depends on geometry and loads. Also,  $K^d(t)$  is a function of time. The contour diagrams, shown in Figure 5, were obtained for values  $|K^d| = 1Pa\sqrt{m}$  and  $F = 45^\circ$ , for the purpose of their comparison with experimental results. Figure 5(b) also presents results of analytical “solution” of Equation (18). This equation, defined by Yang, Suo and Shih (1991), until now was not solved in analytical form. In work by Lambros and Rosakis (1995a) only the numerical solution of Equation (18) was presented. Comparison of those solutions with one presented in Figure 5(b), shows the good agreement between them. Solving Equation (17) was not, until now, found in literature in the analytical form, but only in numerical one.

In Figure 5 are presented results of simulation by *Mathematica* of both Equations (17) (Figure 5(a)) and (18) (Figure 5(b)), for the same crack tip speed  $v = 720$  m/s. The difference in appearance of the two fields is obvious.

For the sake of comparison in Figures 6(a) are given contours that represent the solution of Equation (17) obtained by *Mathematica* simula-

tion and solution of Yang, Suo and Shih (1991), Equation (18). Through this comparison can be noticed that Equation (18), which represents the  $K^d$  dominated field, cannot be used for analysis of the stress field near the tip of a non-uniformly propagating crack. Equation (18) offers satisfactory results only in the immediate vicinity of the crack tip. For the far field (further away from the tip), its characteristics also depend on terms that contain other powers of  $r$  (not only  $r^{1/2}$ ). Since those terms are not included in Equation (18), it cannot satisfactorily describe the field away from the tip. On the other hand, the crack tip stress field obtained by Equation (17), which contains all the significant terms, exhibits the same characteristics as the experimental one. Furthermore, all the field characteristics are very well described by Equation (17) even at distances far away from the crack tip. Thus, Equation (17) describes the complete stress field. This proves that the  $K^d$  dominated field cannot be applied for cases when acceleration exists. Thus, for the exact determination of fracture parameters it is necessary to apply the whole expression. Here one understands that, by Equation (17), which represents the result of the asymptotic analysis of the non-uniform crack growth, the stress field around the crack tip that propagates non-uniformly, can be better described then by Equation (18).

The interferograph obtained in real time, with high-speed photography, taken from literature, Lambros and Rosakis (1995b), is used for an illustration of exceptionally well agreement of analytical results and experimental data. Results obtained by application of *Mathematica* programming package to solving of Equation (17) are "drawn over" that interferograph, in Figure 6(b). The crack tip speed for both cases was 720 m/s. Considering this Figure, it can be concluded that the complete Equation (17), as analyzed in this paper, has to be used in order to adequately describe the stress fields to which correspond high accelerations. In work by Liu, Lambros and Rosakis (1993) the similar comparison was attempted. Over the same interferograph, the contours were drawn obtained by their numerical simulation of Equation (17) (Figure 16 in their paper). They also came to the same conclusion that the whole expression has to be used, i.e., Equation (17) and not (18). However, the results of analytical simulation by *Mathematica* seem to "fit" better to experimental data, than the numerical ones.

Figure 7 offers yet another comparison of results obtained by applica-



tion of Equation (17) and optical interferograph for bimaterial combination Homalite-100/Al. The good agreement of theoretical and experimental data is again confirmed. This also supports the previous conclusion for necessity of application of the complete Equation (18).

Considering the possibilities offered by the *Mathematica* programming package, the further simulations were performed and results are presented in Figure 8, where the stress field around the crack tip is shown for different values of the crack tip speed.

The contour diagrams shown in Figure 8 were obtained for values of  $|K^d| = 1Pa\sqrt{m}$  and  $\Phi = 45^\circ$  and different values of the crack tip speed. From Figure 8 one can see that orientation of the stress field depends on the crack tip speed. This influence is due to the term  $\varepsilon \ln r_\lambda$  in the argument of the sine and cosine terms in equation (17). This term also has influence on change of the phase angle  $\Phi$ . In previous considerations the complex stress intensity factor was not considered as a function of the crack tip speed, but it was being considered as constant. Its value also depends on the chosen sample geometry and applied load.

In Figure 8 one can also notice that the "rings" around the crack tip change their magnitude and orientation with the variation of the crack tip speed, what implies that there are changes in the stress field that surrounds the crack tip. On the other hand, when the crack growth speed is constant, those rings that surround such a crack do not change significantly with time. The consequence of this remark is that some fundamental physical variables, like the stress and the crack surfaces displacement, have to remain constant during the crack growth phase.

From the asymptotic analysis of Yang et al. (1991), the crack surfaces displacements are:

$$\begin{aligned} \delta_1(r) &= \frac{h_{21}}{ch(\pi\varepsilon)} \sqrt{\frac{2r}{\pi}} \frac{|K^d|}{\sqrt{1+4\varepsilon^2}} \frac{1}{\eta} \sin(\Phi + \varepsilon \ln r - \arctg(2\varepsilon)) \\ \delta_2(r) &= \frac{h_{21}}{ch(\pi\varepsilon)} \sqrt{\frac{2r}{\pi}} \frac{|K^d|}{\sqrt{1+4\varepsilon^2}} \cos(\Phi + \varepsilon \ln r - \arctg(2\varepsilon)) \end{aligned} \quad (19)$$

Each of these two displacements in equation (19) depends on  $|K^d|$ , but their ratio is a function only of  $\Phi$  and  $v$ . If one assumes that the ratio  $\delta_1/\delta_2$  remains constant during the crack propagation (and this assumption is plausible taking into account the considerations related to Figure 8), for example  $C_1$ , at a constant distance  $a$  behind the crack tip, then one can write:

$$\left. \frac{\delta_1}{\delta_2} \right|_{r=a} = C_1 = \frac{1}{\eta} \operatorname{tg}(\Phi + \varepsilon \ln r - \operatorname{arctg}(2\varepsilon)) \quad (20)$$

or solving for  $\Phi$ :

$$\Phi = \Phi(v) = \operatorname{arctg}(\eta(v)C_1) + \operatorname{arctg}(2\varepsilon(v)) - \varepsilon(v) \ln a. \quad (21)$$

During the crack propagation the ratio remains  $\delta_1/\delta_2$  constant. When  $C_1 = -0.3$  it means that the magnitude of crack opening is 3.3 times larger than the crack surfaces shear. Based on this, one can conclude that, for the given distance behind the crack tip, the crack opening mode (Mode I) is dominant during the crack growth. For  $C_1 = -3$  the value of shear is 3 times larger than the crack opening behind the crack tip, at a distance  $a = 2$  mm.

In Figure 9 is presented the dependence of  $\Phi$  on  $v$  for two different values of constant  $C_1$  and for  $a = 2$  mm, obtained by applying *Mathematica*.

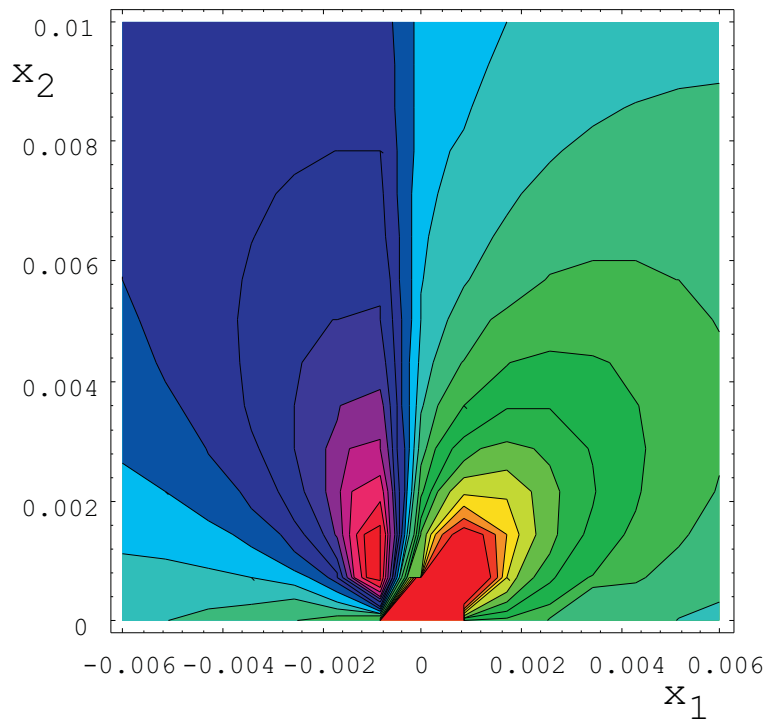
However, the magnitude of the stress field that surrounds the crack tip primarily depends on the value of the complex stress intensity factor  $|K^d|$ . Thus, one should obtain the relationship between  $|K^d|$ ,  $v$  and  $\Phi$ . For this purpose, it is assumed that the value of the crack opening has the constant value,  $C_2$  at the same distance  $a$  from the crack tip. From the second of equations (19), this assumption can be written as:

$$\delta_2(a) = \frac{h_{21}}{ch(\pi\varepsilon)} \sqrt{\frac{2a}{\pi}} \frac{|K^d|}{\sqrt{1+4\varepsilon^2}} \cos(\Phi + \varepsilon \ln a - \operatorname{arctg}(2\varepsilon)) = C_2, \quad (22)$$

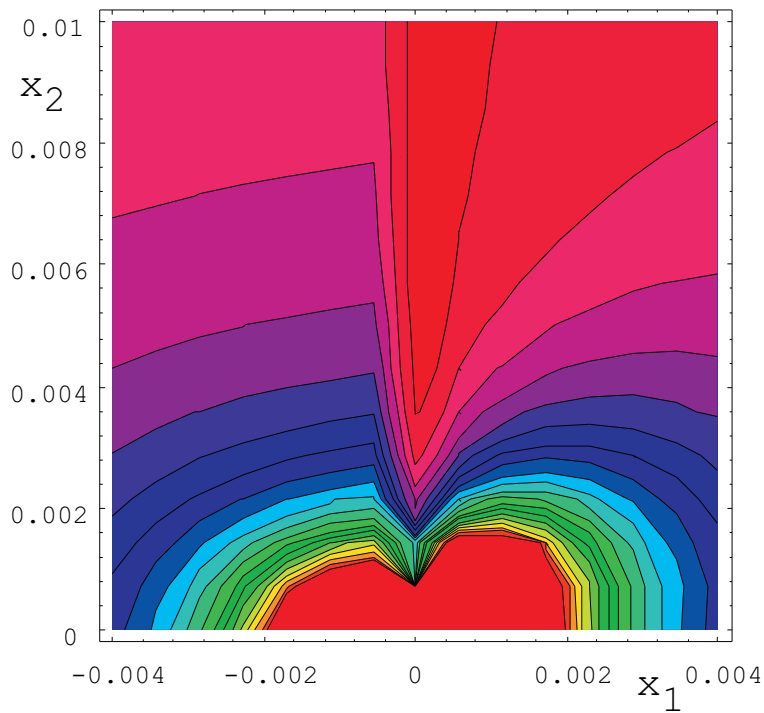
or, solving for  $|K^d|$ :

$$|K^d| = C_2 \frac{ch(\pi\varepsilon)\sqrt{1+4\varepsilon^2}}{h_{21}} \sqrt{\frac{\pi}{2a}} \frac{1}{\cos(\Phi + \varepsilon \ln a - \operatorname{arctg}(2\varepsilon))}. \quad (23)$$

Equation (23) represents the relationship between  $|K^d|$ ,  $v$  and  $\Phi$ , with parameters  $C_2$  and  $a$ .

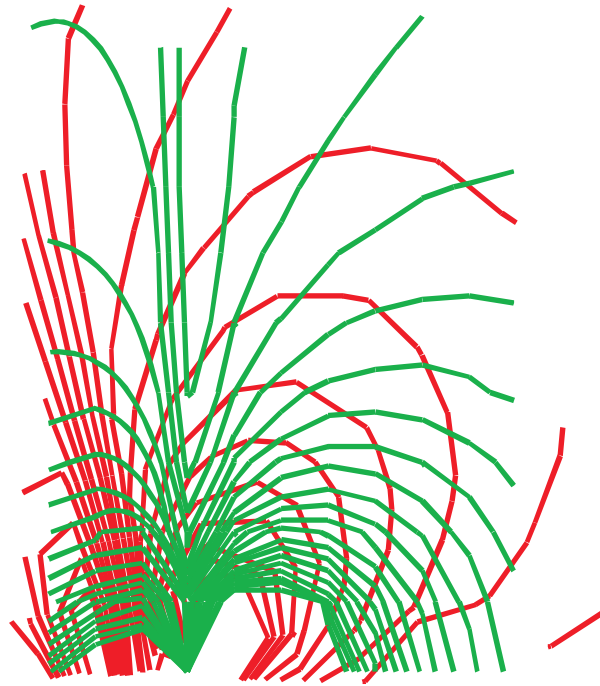


(a) According to Equation (17)

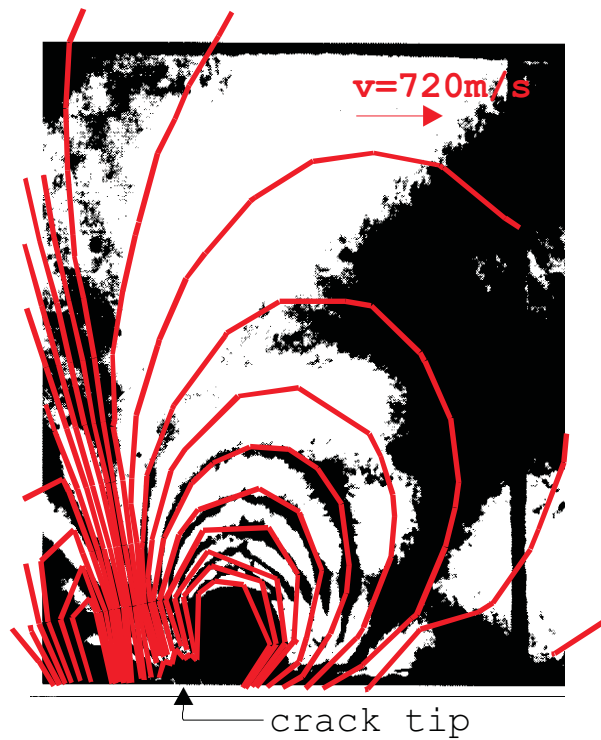


(b) According to Equation (18).

Figure 5: Results of asymptotic analysis of the crack growth for bimaterial combination PMMA/steel, for crack tip speed  $v = 720$  m/s

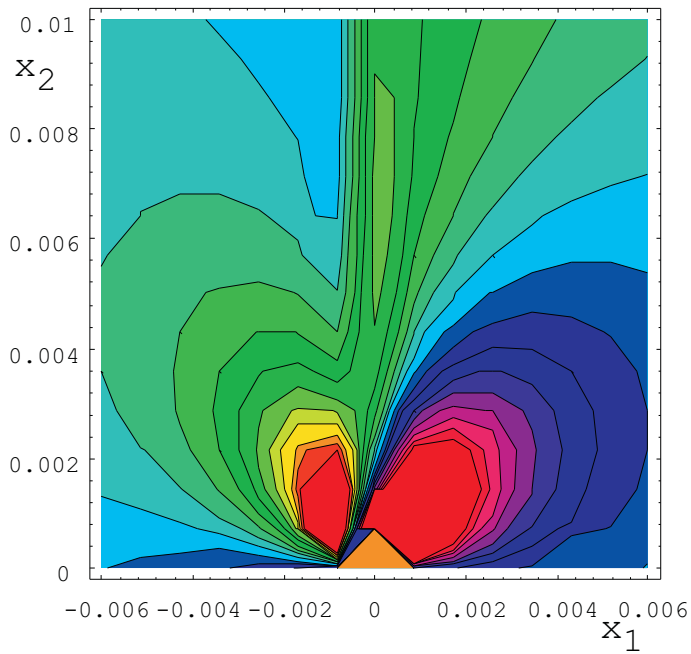


(a) Contours that represent the solution of Equation (17) obtained by *Mathematica* simulation (in red) and solution of Yang, Suo and Shih (1991) (in green)

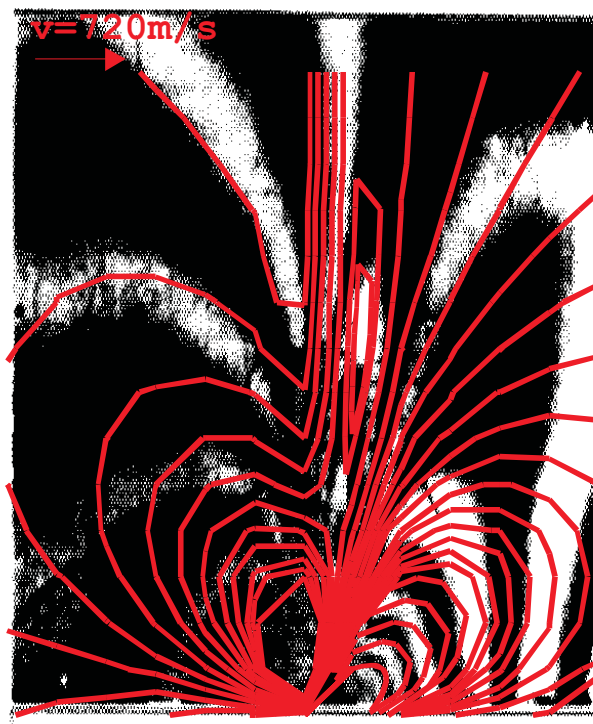


(b) Interferograph obtained for the dynamic crack growth along the PMMA/ steel interface for the crack tip speed  $v = 720$  m/s, Lambros and Rosakis (1995b), together with contours (in red) that represent the solution of Equation (17) obtained by *Mathematica* simulation.

Figure 6:



(a) Results of asymptotic analysis of the crack growth for bimaterial combination Homalite -100/Al according to Equation (17) for crack tip speed  $v = 720$  m/s



(b) Interferograph obtained for the dynamic crack growth along the Homalite -100/Al interface subjected to impact load, Singh et al. (1997)), together with contours (in red) that represent the solution of Equation (17) obtained by *Mathematica* simulation.

Figure 7:

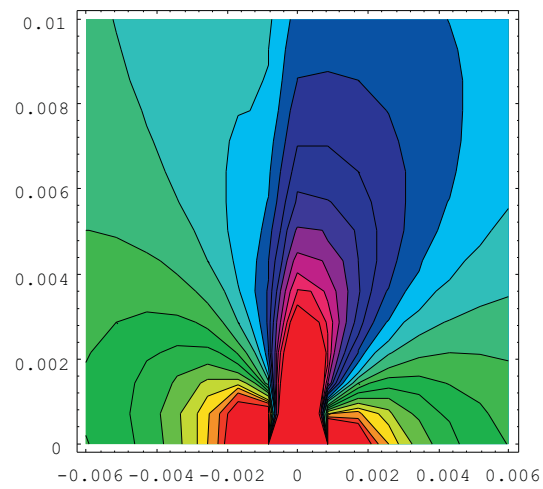
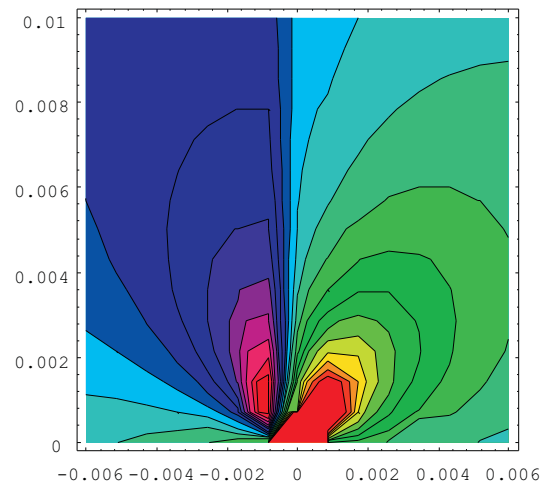
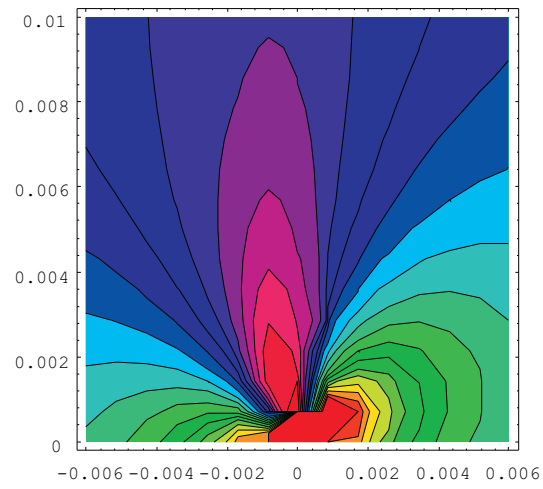


Figure 8: Results of the asymptotic analysis of the dynamic crack propagation for the material combination PMMA/steel according to equation (17) for different values of the crack tip speed

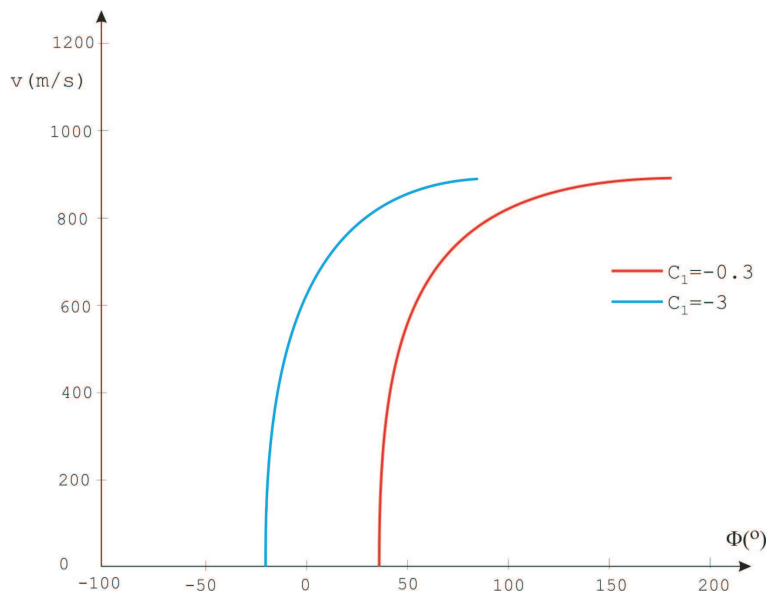


Figure 9: Dependence of the phase angle  $\Phi$  on the crack tip speed  $v$ .

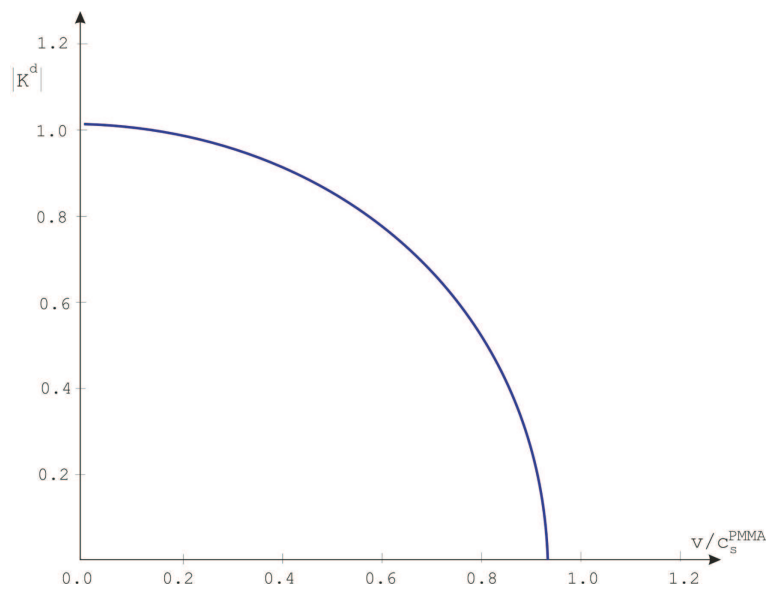


Figure 10: Dynamic stress intensity factor as a function of the crack tip speed

If one substitutes equation (21) into (23), the relationship between  $|K^d|$  and  $v$  is obtained as:

$$|K^d| = C_2 \frac{ch(\pi\varepsilon)\sqrt{1+4\varepsilon^2}}{h_{21}} \sqrt{\frac{\pi}{2a \cos(\arctg(C_1\eta))}}. \quad (24)$$

From equation (24) can be seen that  $|K^d|$  depends on both  $C_1$  and  $C_2$ . The dependence of  $|K^d|$  on  $v$  for the value of parameter  $C_2=1$  is shown in Figure 10. The diagram is also drawn by application of *Mathematica*.

Based on Figures 9 and 10, it can be seen that the crack propagates dynamically across the bimaterial interface until the ratio of the values of opening and shear, for the certain distance behind the crack tip remains constant.

The exact causes of the crack initiation determine the correct crack profile, i.e., the constants  $C_1$  and  $C_2$ . The relationship between  $\Phi$  and  $v$  is such that  $\Phi$  remains approximately constant for the lower values of  $v$ , as can be seen from Figure 9. This is physically justified, since the material inertia can not have the strong influence for the small crack tip speeds.

## 6 Conclusion

The aim of this paper was to present a different approach to asymptotic analysis of the strain field around a crack that is propagating dynamically along a bimaterial interface. The previously offered solutions by Yang, Suo and Shih (1991) (*YSS*) and Liu, Lambros and Rosakis (1993) (*LLR*) were compared with each other. The main point was to illustrate the possibilities of application of the *Mathematica* programming routine in this analysis. As a conclusion from results obtained by *Mathematica* simulations of both solutions, and their comparisons with available experimental data, it is quite obvious that the whole expression for the first stress invariant, given by Liu, Lambros and Rosakis (1993) has to be applied.

The *YSS* solution only refers to the first term of the *LLR* equation. It offers satisfactory results for the field only in the immediate vicinity of the crack tip. For the far field, whose characteristics also depend on terms that contain other powers of  $r$  (not only  $r^{1/2}$ ) this solution is not adequate. Since those terms are not included in the *YSS* equation, it cannot satisfactorily describe the field away from the tip, while the *LLR* equation



describes the complete stress field. This proves that the  $K^d$  dominated field cannot be applied for cases when acceleration exists. The simulations obtained by the *Mathematica* programming routine were superior over the corresponding numerical solutions of the *LLR* expression, what was shown by comparison to the experimental results.

Considering the possibilities offered by the *Mathematica* programming package, the further simulations were performed and the stress field around the crack tip was calculated for different values of the crack tip speed. It was shown that orientation of the stress field depends on the crack tip speed. This influence is due to the term  $\varepsilon \ln r \lambda$  in the argument of the sine and cosine terms in the *LLR* equation. This term also influences the change of the phase angle  $\Phi$ .

In previous considerations the complex stress intensity factor was not considered as a function of the crack tip speed, but it was being considered as constant. Its value also depends on the chosen sample geometry and applied load. However, the "rings" of the stress field around the crack tip, on the diagram, change their magnitude and orientation with the variation of the crack tip speed, what implies that there are changes in the stress field that surrounds the crack tip. When the crack growth speed is constant, those rings that surround such a crack, do not change significantly with time. This means that some fundamental physical variables, like the stress and the crack surfaces displacements, have to remain constant during the crack growth phase.

During the crack propagation the ratio of the crack surfaces displacements  $\delta_1/\delta_2$ , remains constant ( $C_1$ ). For instance, when  $C_1 = -0.3$  it means that the magnitude of crack opening is 3.3 times larger than the crack surfaces shear. Based on this, one can conclude that, for the given distance behind the crack tip, the crack opening mode (Mode I) is dominant during the crack growth. For  $C_1 = -3$  the value of shear is 3 times larger than the crack opening behind the crack tip, at a distance  $a = 2$  mm.

The crack propagates dynamically across the bimaterial interface until the ratio of the values of opening and shear, for the certain distance behind the crack tip remains constant.

The magnitude of the stress field that surrounds the crack tip primarily depends on the value of the complex stress intensity factor  $|K^d|$ , which was expressed in terms of crack tip speed  $v$  and phase angle  $\Phi$  and depends on both ratio of the crack surfaces displacements  $\delta_1/\delta_2$  ( $C_1$ ) and some

constant value of the COD ( $C_2$ ).

The exact causes of the crack initiation determine the correct crack profile, i.e., the constants  $C_1$  and  $C_2$ . The relationship between the phase angle  $\Phi$  and crack tip speed  $v$  is such that  $\Phi$  remains approximately constant for the lower values of  $v$ . This is physically justified, since the material inertia can not have the strong influence for the small crack tip speeds.

### Acknowledgements

Authors of this work would like to express their appreciation and gratitude to Professor James R. Rice of SEAS, Harvard University, for being so kind in reading this text and for his most useful and adequate suggestions for its improvements.

This work was partially done while the first author was a visiting professor at Faculty of Civil Engineering, University of Zilina, Slovak Republic, on the SAIA grant of the Slovakian Ministry of Education.

### References

- [1] \*Williams, M. L., (1959), "The stresses around a fault or crack in dissimilar media", Bull. of the Seism. Soc. of America, **49**, pp. 199-204.
- [2] Sih, G. C. and Rice J. R., (1964), "Bending of plates of dissimilar materials with cracks", J. Appl. Mech., **31**, pp. 477-482.
- [3] Rice, J. R. and Sih G. C., (1965), "Plane problems of cracks in dissimilar media", J. Appl. Mech., **32**, pp. 418-423.
- [4] Erdogan F., (1965), "Stress Distribution in Bonded Dissimilar Materials with Cracks", J. Appl. Mech., **32**, pp. 403 - 410.
- [5] England A.H., (1965), "A Crack between Dissimilar Media", J. Appl. Mech., **32**, pp. 400 - 402.
- [6] \*Malyshev, B. M. and Salganik R. L., (1965), "The strength of adhesive joints using the theory of crack", Int. J. of Fract. Mech. **1**, pp. 114-128.

- [7] Rice J. R., (1988), "Elastic fracture mechanics concepts for interfacial cracks" J. Appl. Mech., **55**, pp. 98 - 103.
- [8] Hutchinson, J. W. and Suo Z., (1992), "Mixed mode cracking in layered materials", Adv. Appl. Mech., 29. pp. 63 - 191.
- [9] Shih, C. F., (1991), "Cracks on bimaterial interfaces: Elasticity and Plasticity aspects", Mat. Science and Engineering, **A143**, pp. 77-90
- [10] Liu C., Lambros J., Rosakis A. J., (1993), "Highly transient elastodynamic crack growth in bimaterial interface: higher order asymptotic analysis and optical experiments", J. Mech. Phys Solids, **41**(12), pp. 1887-1954.
- [11] Tippur H. V. and Rosakis A. J., (1991), "Quasi-static and dynamic crack growth along bimaterial interfaces: A note on crack-tip field measurements using coherent gradient", Int. J. of Fracture, **48**, pp. 243-251.
- [12] Rosakis A. J., Lee Y. J., Lambros J., (1991), "Dynamic Crack Growth in Bimaterial Interfaces", Experiments in Micromechanics of Failure Resistant Materials, AMD-Vol. **130**, ASME, pp. 17-23.
- [13] Yang, W., Suo Z. and Shih C. F., (1991), "Mechanics of dynamic debonding", Proc. R. Soc. London. **A 433**, pp. 679-697.
- [14] Lo, C. Y., Nakamura, T. and Kushner, A., (1994), "Computational Analysis of Dynamic Crack Propagation along a Bimaterial Interface", Int. J. Solids Structures, 312, pp. 145-168.
- [15] \*Freund, L.B., (1990), Dynamic Fracture Mechanics, Cambridge University Press, Cambridge.
- [16] \*Freund, L. B. and Rosakis A. J., (1992), "The structure of near tip field during transient elastodynamic crack growth", Journal of the Mechanics and Physics of Solids, **40**, pp. 699-719.
- [17] \*Liu C. and Rosakis A. J., (1994), "On the Higher Order Asymptotic Analysis of a Non-Uniformly Propagating Dynamic Crack along an Arbitrary Path", J. Elasticity, **35**, pp. 27-60.

- [18] Singh R. P., Lambros J., Shukla A., Rosakis A. J., (1997), "Investigation of the mechanics of intersonic crack propagation along a bimaterial interface using coherent gradient sensing and photo elasticity", Proc. R. Soc. Lond. **A 453**, pp. 2649-2667.
  - [19] Veljkovic, J.M., (1998), "Analysis of the Problem of the Crack Growth along an Interface between Two Metal Materials", M. Sc. Thesis, Faculty of Mechanical Engineering, Kragujevac, Serbia.
  - [20] Veljkovic, J.M., (2001), "Solving of the Crack Problem on the Interface between Two Materials", Ph.D. Thesis, Faculty of Mechanical Engineering, Kragujevac, Serbia.
  - [21] Nikolic R. and J. Veljkovic, (2002), "Stress Distribution around the Tip of the Dynamically Propagating Interfacial Crack", Proc. ICNM-IV, Shanghai, P. R. China.
  - [22] Nikolic R. and J. Veljkovic, (2004), "Some problems of cracks on bimaterial interface", in "From fracture mechanics to structural integrity assessment", in IFMASS 8, Monograph, S. Sedmak and Z. Radakovic, eds., Belgrade, Serbia, pp. 61-82.
  - [23] Anderson, T.L., (1991), Fracture Mechanics - Fundamentals and Applications, CRC Press, Boston.
  - [24] Lambros J. and Rosakis A. J., (1995a), "Development of dynamic decohesion criterion for subsonic fracture of the interface between two dissimilar materials", Proc. R. Soc. London. A **451**, pp. 711-736.
  - [25] Lambros J. and Rosakis A. J., (1995b), "Dynamic decohesion of bimaterials: Experimental observations and failure criteria", Int. J. Solids Structures, 32, pp. 2677-2702.
- 

\*Reference quoted in Liu, Lambros and Rosakis (1993).

Submitted on August 2009, revised on December 2009.

### **Nov pristup analizi dinamikog rasta prsline na bimaterijalnom interfejsu**

U ovom radu je prikazan nov pristup asimptotskoj analizi polja napona i deformacije oko vrha prsline koja dinamički propagira duž bimaterijalnog interfejsa. Kroz asimptotsku analizu problem je sveden na rešavanje Riemann-Hilbert-ovog problema, ime se dobija potencijal relativne deformacije koji se koristi za određivanje polja deformacije oko vrha prsline. Razmatrano je polje oko prsline koja propagira dinamički brzinom koja se nalazi između nule i brzine smičajnog talasa manje krutog od dva materijala, koji su spojeni interfejsom. Korišćenjem novog pristupa u asimptotskoj analizi polja deformacije oko vrha dinamički rastue prsline i mogućnosti koje pruža programski paket Mathematica, dobijeni su rezultati koji su upoređeni sa eksperimentalnim i numeričkim rezultatima poznatim iz literature. Ova poređenja pokazuju da mora da se koristi potpuni izraz dobijen asimptotskom analizom, a ne samo njegov prvi član kako je radjeno u ranijim analizama.